

RESEARCH PAPER

Effect of Textural Properties of Y, ZSM-5 and Beta Zeolites on Their Catalytic Activity in Catalytic Cracking of a Middle Distillate Cut Named RCD

Faezeh Mirshafiee¹, Ramin Karimzadeh¹, Reza Khoshbin²

¹ Faculty of Chemical Engineering, Tarbiat Modares University, Tehran, Iran

² Buin Zahra Higher Education Center of Engineering and Technology, Imam Khomeini International University, Qazvin, Iran

ARTICLE INFO

Article History:

Received 2021 March 12

Revised 2021 August 22

Accepted 2021 November 4

Keywords:

Catalytic cracking
heavy hydrocarbons
zeolite Y
zeolite Beta
Zeolite ZSM-5

ABSTRACT

In the present study, the performance of three catalysts containing Y, ZSM-5 and Beta zeolite in the catalytic cracking of a kind of middle distillate cut named "RCD" has been studied. The catalysts were characterized by XRD, FTIR, SEM, N₂ adsorption/ desorption and NH₃-TPD techniques. Furthermore, deactivated catalysts in terms of type and amount of deposited coke were analysed. Results of catalytic tests showed that Y zeolite performed better and it decreased viscosity and density of liquid product by 35% and 3% respectively. This good operating was due to the high surface area (812m²/gr) and higher acidic sites amounts (1.8 mmol NH₃/gr) which gives the heavy molecules better accesibility to active acid sites. But more cokes have deposited on Y zeolite which was 50% lower for Beta and ZSM-5 zeolites. Finally, it can be concluded that the ultimate performance of catalysts in catalytic cracking is influenced by the synergetic effects between the pore structure and acidity.

How to cite this article

Mirshafiee F, Karimzadeh R, Khoshbin R, Effect of Textural Properties of Y, ZSM-5 and Beta Zeolites on Their Catalytic Activity in Catalytic Cracking of a Middle Distillate Cut Named RCD, Journal of Oil, Gas and Petrochemical Technology, 2021; 8(2): 60-74. DOI:10.22034/JOGPT.2022.273313.1092.

1. Introduction

The decline in traditional light oil resources on one side and the rising requirement for strategic products like gasoline and diesel oil on the other hand, forced researchers to do research on catalytic cracking of heavy oil. Heavy oil and residual distillate like vacuum residue, atmospheric tower residue, etc are very viscous and contain complex molecules and impurities like asphaltene, sulfur and nitrogen, which may cause problems during the process[1]. So, in these processes it is important to select the appropriate catalyst to be able to convert low value-added heavy crudes into high-value

added materials. Among the various catalysts, zeolite catalysts with high surface area, high thermal stability and selectivity to specific products are of interest [2]. Zeolites are crystalline aluminosilicates composed of three-dimensional networks that are interconnected by sharing oxygen atoms. Eventually, as these networks and structural units come together, the crystalline structure of the zeolite consists of one, two or three-dimensional channels formed[3]. The three zeolites containing ZSM-5, Y and Beta are among the most popular zeolitic catalysts used in the industry[4]. In catalytic cracking of heavy ends, a lot of scientific research was done on these three zeolites [5–9]. Considering the importance of choosing the best catalyst,

comparing these three zeolites can be very appealing. However, there are only a few studies regarding the comparing these important zeolite in catalytic cracking. In addition, in many FCC applications, one of these three zeolites is added to the other as an additive, so it is necessary to know how each of these catalysts behaves in the catalytic cracking process.

Na-Y zeolite is a molecular sieve from the faujasite zeolite family that is widely used in the fluidized bed catalytic cracking, Organic materials adsorption, etc which its structure is shown in Figure 1(a) [10]. For the first time, the commercial synthesis of Na-Y zeolite was carried out by Breck in 1964. He stated that the conversion of the two zeolites X and Y to each other occurs at a ratio of Si/Al = 1.5, where the zeolite with Si/Al less than 1.5 is known as X zeolite and the Si/Al ratio above 1.5 is known as Y zeolite[11]. This zeolite with an average pore size of 0.74 nm considered as a large pore zeolite[12]. Due to the high surface area, strong acidity and low cost of synthesis, numerous researchers have used this zeolite in cracking of heavy oil [13]. Qin et al. by merging desilication and dealumination on Y zeolite, they were able to produce mesoporous ultra-stable Y zeolite, which increases the gasoline selectivity up to 3%, light cycle oil increased by 2% and coke decreased by 2% in heavy oil cracking [14] Lee et al. used Y zeolite to convert heavy oils, which hierarchical samples had high selectivity to liquid products[15]. Oruji et al. applied the simultaneous precipitation of lanthanum oxide with the help of ultrasound waves in upgrading of massive hydrocarbons which reduced the acidity strength of zeolite so eventually increase the catalyst lifetime [16]. Aghaei et al. also investigated the catalytic performance of prepared Y zeolite in catalytic cracking of Iso-diesel which the results showed that the best conversion about 70% and selectivity to kerosene about 45% was obtained in samples treated with CaCO₃ alkaline agent [17]modified Y zeolite with high catalytic activity and long lifetime was successfully prepared using sequential steam-alkali-acid treatments. Different alkali agents (NaOH, Na₂CO₃ and CaCO₃).

Beta zeolite,with BEA structure which is shown in Figure 1(b), has an average pore sizes of 0.67 nm which is known as a medium-pore zeolite [18]. This zeolite was first synthesized by

Wadlinger et al. in 1967 in an alkaline environment in the presence of TEOH by hydrothermal method[19]. Because of its large-pore channel system, good acidity and good hydrothermal stability, Beta zeolite has attracted many researchers attention [20]. Corma et al. observed when Beta zeolite was used in the cracking of gas oil, more heavy compounds of the coke family were produced compared with USY, and Y zeolite was more active than Beta zeolite. Whereas for n-heptane cracking, the Beta zeolite is more active than the Y zeolite with a similar ratio of Si/Al, which is due to the existence of channels with different dimensions in the Beta zeolite[21]. Qi et al. studied the catalytic cracking of 1,3,5 tri isopropyl benzene on mesoporous Beta zeolite which the mesoporous Beta because of the presence of the hierarchical porosity exhibits high catalytic activity compared with the conventional microporous Beta [4]. Smirniotis et al. by adding Beta zeolite and ZSM-5 as an additives to the conventional cracking catalysts, Faujasite, concluded that Beta zeolite was more selective to four-membered hydrocarbons. That's why Beta zeolite as an additives are more appealing than the ZSM-5, which adds to its popularity as a cracking catalyst[22].

ZSM-5 zeolite is a molecular sieve of the MFI zeolite family which its structure is shown in Figure 1(c). This zeolite by pore sizes in the range of 5.5Å has a silica-rich structure which first synthesized in 1965 by Landolt et al. [23]. Due to its uniform channel structure, high acidity, high thermal and hydrothermal stability, ZSM-5 is one of the most successful zeolite in catalytic cracking [24]. Awayssa et al. to maximize the yield of light olefins resulting from the catalytic cracking of heavy oil, they added an amount of ZSM-5 zeolite to the USY catalyst (25% by weight) in FCC reactors [25]propylene. Ishihara et al. applied zeolite ZSM-5 in catalytic cracking of VGO that its mesoporous type created a large number of branched compound that increased the products octane number [26]. Safari et al. employed alkaline treatment to induce mesopores in ZSM-5 catalyst to improve molecular diffusion in the cracking/co-oxidation of heavy oil. They observed by applying air stream, the conversion of heavy oil on alkaline treated ZSM-5 was improved from 45.7% up to 58.1% [27].

As the selection of the appropriate catalyst for converting low value- heavy crudes into high-val-

* Corresponding Author Email: Ramin@modares.ac.ir
Email: r.khoshbin@bzeng.ikiu.ac.ir

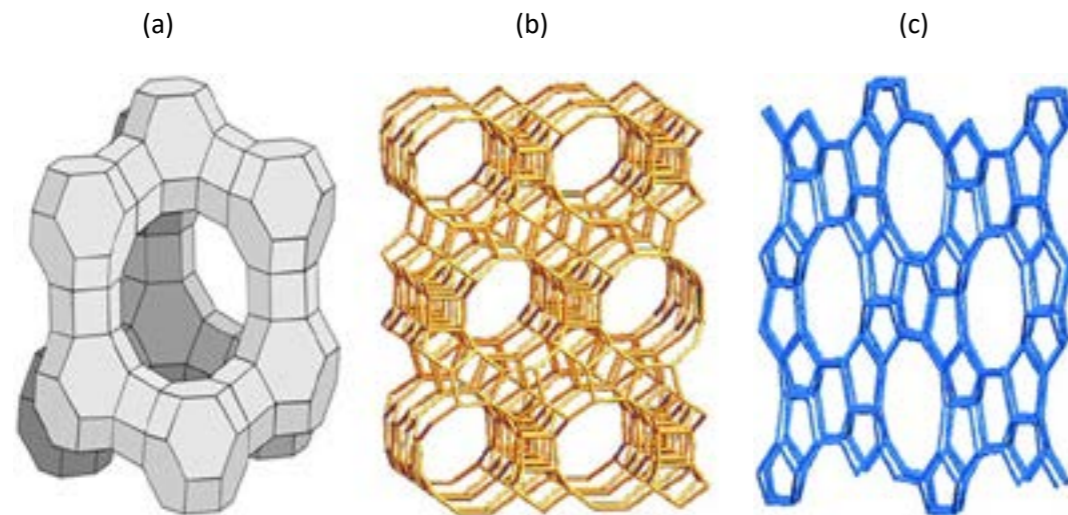


Figure 1. The structure of three zeolites containing Y(a) [28] , Beta(b) [29] and ZSM-5(c) [30] zeolites

ue materials is very important, herein, cracking of RCD over three zeolite containing Y, ZSM-5 and Beta zeolites as a solid acid catalyst, were comparatively investigated. RCD is the name of a cut that is derived from the RCD unit, which stands for Reduced Crude Desulfurization and plays the role of reducing sulfur.

2. Research method

2.1. Materials

Three Commercial zeolites was provided from different companies: Zeolite NH_4 -Beta with $\text{SiO}_2/\text{Al}_2\text{O}_3 = 25$ from Zeolyst International Company (CP814E), Y zeolite ($\text{SiO}_2/\text{Al}_2\text{O}_3 = 5.2$) in sodium form from Naika company (china) and Na-ZSM-5($\text{SiO}_2/\text{Al}_2\text{O}_3 = 38$) from Chemist company. Furthermore, other raw materials were ammonium nitrate NH_4NO_3 (Ghatran

shimi) for converting zeolite into H-form, de-ionized water to create a dilute environment and a middle distillate cut(RCD) as feed in catalytic cracking tests which was brought from Arak refinery(Iran).

2.2. Catalysts preparation procedures

To obtain protonic form of as-received Beta zeolite, it was calcined in furnace at 550°C for 4 hr in air stream. This sample was labeled Beta. To convert Na-Y and Na-ZSM-5 to protonic form, according to Figure 2, samples were treated with 1 M NH_4NO_3 solution, at 80°C for 3 hr, and it was filtered and finally dried at 100°C for 12 hr. This treatment repeated two more times to completely replace of Na^+ ions with NH_4^+ . Then this zeolites calcined at 550°C during 4 hr under air stream. This samples were labeled Y and ZSM-5.

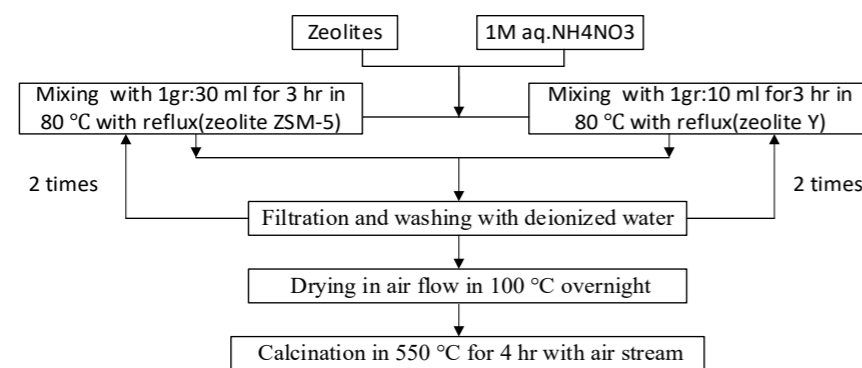


Figure 2. Schematic flow chart of Catalysts preparation

2.3. Applied characterization techniques

2.3.1. Catalyst characterization

In order to investigate the crystallinity and phase purity of samples, their XRD(X Ray Diffraction) patterns using a BRUKER diffractometer, model D8 ADVANCE ,Germany and $\text{CuK}\alpha$ radiation ($\lambda = 1.54056 \text{ \AA}$) at 40 kV and 40 mA were recorded. Scans were performed in the range of $2\theta = 5\text{-}80^\circ$ and then the resulted patterns were compared to the standard patterns which reported in JCPDS data base files. For determining surface functional groups of nanocatalysts, FTIR(Fourier Transform Infrared) alalysis of catalysts performed by PerkinElmer IR spectrophotometer version 10.03.06, USA, using KBr pressed disk technique within the range of $400\text{-}4000 \text{ cm}^{-1}$. To obtain information about the morphologies and size of the particles , scanning electron microscopy (SEM) analysis were carried out by VEGA\TESCAN-LMU model apparatus. For better electrical conductivity, before the characterization, a very small amount of gold was layered on the samples. The textural properties of samples were measured by N_2 adsorption-desorption analysis by ASAP 2020 V3.03 G Plus instrument. The specific surface area of samples were recorded by BET (Brunauer, Emmett and Teller) method. The acid properties of the samples were also characterized by a Temperature Programed Desorption of NH_3 (NH_3 -TPD) method on an instrument made by Micromeritics (USA).

2.3.2. Product and coke characterization

Kinematic viscosity, density and refractive index of the liquid products were measured by a Liquid viscometer according to ASTM D47042, a pycnometer (Isolab, Germany) according to ASTM D1480 standard and a refractometer NAR-1T Liquid (Atago, Japan) by ASTM D1218 respectively.

For determining some properties of feed and product like molecular weight and H/C (hydrogen-to-carbon atomic ratio), Riazi equation was applied [31]:

$$P = a \times \exp(b \times vis_{37,8^\circ\text{C}} + c \times I + d \times (1) \quad (1)$$

$$vis_{37,8^\circ\text{C}} \times I \times (vis_{37,8^\circ\text{C}})^e \times (I)^f$$

Where, P can be either Molecular Weight (gr/mol) or H/C (hydrogen to carbon atomic

ratio). , as defined below, is an index called "refractive index" that the constants of this equation exposed by mentioned references.

$$I = \frac{n^2 - 1}{n^2 + 1} \quad (2)$$

After the reactions, amounts of coke deposited on zeolites were determined by putting samples in the air-supplied furnace at 550°C for about 4 h. In which, due to the burning of coke, a decrease in the mass of the sample will occurred, which can be a measure of the amount of deposited coke . Based on the literature, the weight losses in the temperature lower than 200°C can be related to the moisture removal [32]. So, we first heated the sample in the furnace up to 200°C , weighed the sample after one hour (case 1), then put the sample back in the furnace and raised the temperature to 550°C and weighed again after 4 hours (case 2). Finally the difference of weight losses of cases one and two is reported as the weight of the accumulated coke. Moreover, spent catalysts were studied by FTIR analyses to study the molecular structure of deposited coke.

2.4. Catalyst performance test

A simple schematic diagram of the lab-scale setup used in this research is shown in Figure 3. Catalyst performance evaluation was performed in a cylindrical stainless steel fixed bed reactor which was installed inside a K-type thermocouple equipped with furnace to supply the reaction temperature. A middle distillate cut from Arak refinery, with the specifications in Table 1, was provided as a feed.

Table 1. RCD Feedstock properties

MW, ($\text{g}\cdot\text{mol}^{-1}$)	161.38
Viscosity at 37.8°C (CSt)	1.914
Density ($\text{g}\cdot\text{cm}^{-3}$)	0.875
Refractive Index	1.474
H/C Atomic ratio	7.24
Nitrogen content (ppmw)	350
Sulphur content (wt%)	0.05
FBP ($^\circ\text{C}$)	330

For each test, 1 gram of shaped catalyst loaded in the middle of the reactor with quartz wool on either side. Nitrogen (50 cc/min), as a carrier gas, was mixed with the feed. When desired temperature of 550°C was reached, the feed was injected by the syringe pump

with the flow of 0.5 gr/min. After the reaction, product that is a combination of gas and liquid, led to the condenser to collect the liquid product while non-condensable gas products burned in flare. After the process, feed stream was interrupted but nitrogen continued to cross the bed for 30 minutes to purge the catalyst bed.

Yield of each product was defined by the following equations :

$$\text{Liquid product yield } (Y_{\text{liquid}}) = \frac{M_{\text{liquid}}}{M_{\text{feed}}} * 100 \quad (3)$$

$$\text{Coke yield } (Y_{\text{coke}}) = \frac{M_{\text{coke}}}{M_{\text{feed}}} * 100 \quad (4)$$

$$\text{Gas product yield } (Y_{\text{gas}}) = 100 - Y_{\text{liquid}} - Y_{\text{coke}} \quad (5)$$

Where "M" is the mass of the components that are written as subscript. Furthermore, after the liquid collection, some of its characteristics like density, refractive index (RI) and viscosity were also measured.

3. Results and Discussion

3.1. Characterization of three zeolites

3.1.1. XRD analysis

The XRD patterns of the three catalysts are presented in Figure 4. Y zeolite with diffraction peaks at $2\theta = 6.3^\circ, 10.3^\circ, 12.2^\circ, 16^\circ, 19.1^\circ, 20.7^\circ, 23.3^\circ, 24.1^\circ, 27.6^\circ$ and 31.4° showed standard XRD patterns of the faujasite structure (JCPDS 01-077-1551).

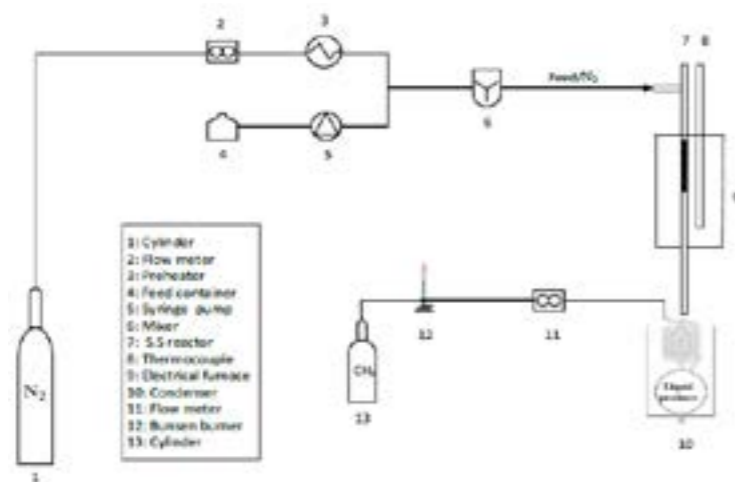


Figure 3. Experimental apparatus for catalytic cracking test of heavy oil

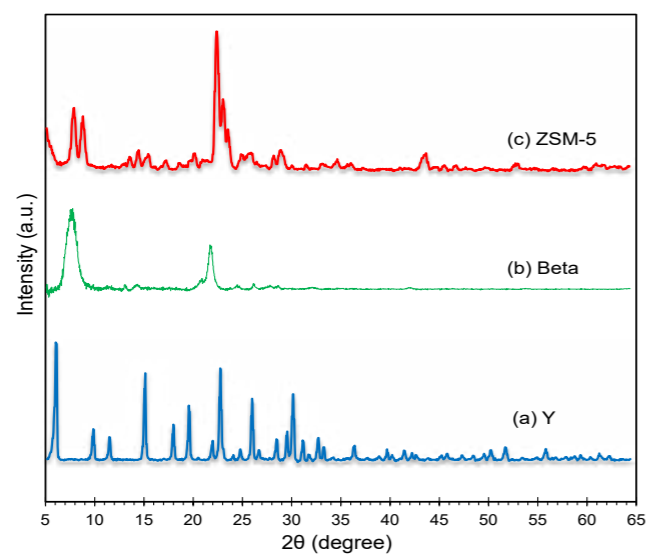


Figure 4. XRD patterns of catalysts: (a) Y, (b) Beta and (c) ZSM-5

XRD pattern of Beta zeolite with prominent peaks at $2\theta = 7.5^\circ$ and 22.4° and ZSM-5 sample with diffraction peaks at $2\theta = 7.99^\circ, 9.14^\circ, 23.21^\circ, 23.65^\circ$ and 24.38° presents typical diffraction pattern of BEA (JCPDS 48-0074) and MFI structure (JCPDS 00-044-0002), respectively.

3.1.2. FTIR analysis

Figure 5 shows the results of the FTIR analysis on three catalysts. FTIR spectra of Y sample represent its faujasite structure. The bands at $448\text{cm}^{-1}, 721\text{cm}^{-1}$ and 994cm^{-1} are referring to the different kinds of T-O-T bending vibration and the band at 570cm^{-1} indicate rings that are specifically present in the micropores of Y zeolite [33].

Moreover, the sharp intense band around 3365cm^{-1} is due to the hydroxyl groups presented in Y zeolite. FTIR spectra of Beta sample represent its BEA structure. Peak at 460cm^{-1} is due to the T-O-T bending mode and the peaks at 522cm^{-1} and 573cm^{-1} are due to the presence of four and five membered rings

of Beta zeolite respectively [34]. FTIR spectra of ZSM-5 sample represent its MFI structure. The bands at 455cm^{-1} is due to the T-O bending vibration and bands at 546cm^{-1} is due to the double 5 ring vibration. In addition, the existence of bands at $794\text{cm}^{-1}, 1086\text{cm}^{-1}$ and 1224cm^{-1} related to the different kinds of symmetric/asymmetric stretch vibration that verifies the ZSM-5 presence [35].

3.1.3. SEM analysis

The result of SEM morphological analysis are displayed in Figure 6. As can be seen, the Y zeolite had an octahedral morphology with well-defined particles assigned to FAU type zeolite which is in line with the results of previous researches [14]. Beta sample presents particles that are generally spherical and elliptical with almost uniform particle sizes as reported in literature [36]. The ZSM-5 sample, as reported in literature, had hexagonal morphology like a coffin with particles length around $4\mu\text{m}$ as shown in Figure 6.(c) [37].

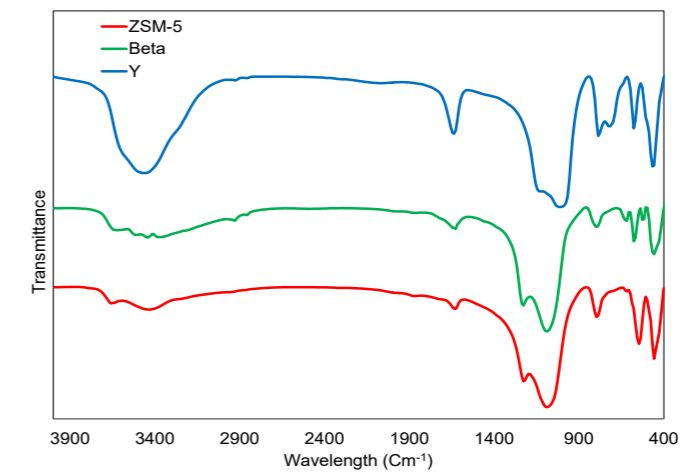


Figure 5. FT-IR spectrum of ZSM-5, Y and Beta zeolites

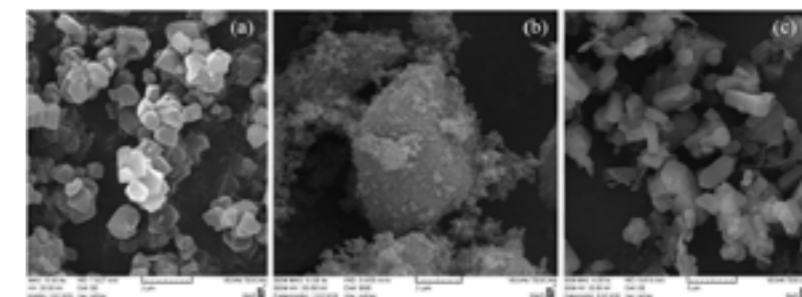


Figure 6. SEM images of Y (a), Beta (b) and ZSM-5 (c)



3.1.4. N₂ adsorption/desorption analysis

Information about the pore specifications of the samples were obtained by N₂ adsorption-desorption analysis. The calculated textural properties are inscribed in Table 2. As it is shown, Beta sample has the highest total pore volume (0.95 cm³/g) and the highest mesoporous volume (0.73 cm³/gr) among the samples. It can be seen that Y zeolite exhibits higher micropore surface areas and micropore volumes compared to other zeolites. Specific surface area affects the adsorption of the reactants on the active sites, so plays a vital role in the progress of catalytic cracking process. But, the synergetic effect between acidity and micro/mesoporous structure and porosity, determine the ultimate performance of catalyst in the catalytic cracking process [38].

The N₂ adsorption/desorption isotherms and pore size distribution of three zeolites are presented in Figure 7. As it is clear, all samples shows a type I adsorption equilibrium curve that is a characteristic of micropores material, and a hysteresis loop for Beta zeolite which is a characteristic of mesopores material. Moreover, the BJH pore size distribution confirmed the existence of these micro/mesopores. The mesopores on Beta zeolite can be attributed to the extraction of aluminum during primary calcination and thus creation of

an empty space in the form of mesopores in the zeolite structure[39].

3.1.5. NH₃-TPD analysis

To examine the acid properties of the synthesized catalysts, ammonia TPD spectra analysis was employed.

As shown in Figure 8, the TPD profile of ZSM-5 sample showed two peaks, in which the peak around 240 °C is assigned to the desorption of NH₃ from weak acid sites and the peak around 470 °C is ascribed to the desorption from strong acid sites. But, the TPD profile of Beta and Y zeolites showed only the peak related to the weak acid sites. Peak position is a measure of the strength of acid site that peak position transition to the lower temperature is a measure of decreased acidity strength. Whereas the amount of acid site is calculated from desorption peak areas[40].

Based on Figure 8, the strength of acid sites increased with the following order: ZSM-5 Beta Y which is in good agreement with those reported in the literature [41] Moreover, the total acid amount increased with the following order: Y ZSM-5Beta which is attributed to the less Si/Al ratio of zeolite Y and its high framework Al amount. As the high acid concentration are favorable for coke formation,so ,more coke is expected to form on Y zeolite.

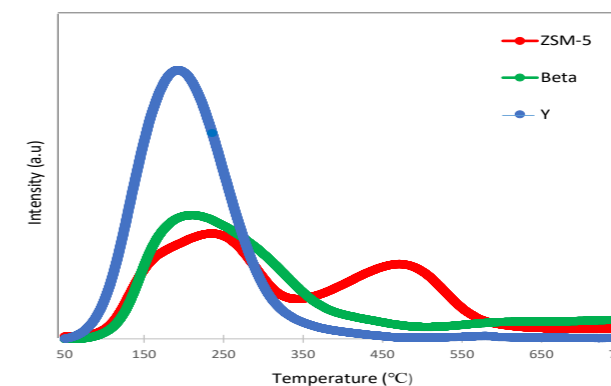


Figure 8. Characterizations of the acidic properties by NH₃-TPD curves

3.2. Comparative performances of three zeolites toward catalytic cracking

Catalytic performance of three zeolites was explored in the manner described in section 2.4. As the catalytic performance depends on the synergetic effect between acidity and micro/mesoporous structure and porosity, therefore a combination of these factors, determine the final performance of catalysts[38].

Cracking activities of three zeolites investigated by the yields of products and liquid product specifications. As we know the aim of catalytic cracking reaction is converting heavy hydrocarbons to the lighter one. It means, the better the cracking reaction, the more gas is produced. So, by measuring the amount of each products, one can compare catalytic activity of different catalysts. In addition, FTIR analysis and weight loss of deactivated catalyst were studied after the process.

3.2.1. Catalytic activity

The activities of catalysts are investigated by RCD as feed and tested for 210 min at 550 under atmospheric pressure. The experimental procedure was repeated at least three times and the average results were reported here. It should be noted that the trend of results has been the same each time. Liquid/gas products yield over this catalysts, are shown in Figure 9 and Figure 10 respectively. By increasing reaction time, the liquid yield of all samples had a rising trend due to the coke formation and catalysts deactivation. During the reaction, the active sites which most of the feed is converted to cracked products on it, covered partially by coke so restricting the accessibility of reactant to active sites and

decreasing catalyst activities. Therefore, after a certain time on stream, liquid production increases and gas production decreases and finally reaches a constant value, which the catalyst activity is reduced and the so-called catalyst is deactivated [42]. All samples had an upward trend in the production of liquid products and downward trend of gaseous product until the end of 210 min time on stream, which means that the catalyst has maintained its relative activity until the last moment. As mentioned above, high yield of gases product and the low yield of liquid product can illustrate higher catalytic activity of the samples, so it seems Y zeolite has a higher catalytic activity. The highest yield of gases product over Y zeolite which shows the higher catalytic activity is due to its higher acidity which are great advantages for catalytic cracking of bulky hydrocarbon. However at the same time, high acidity accelerates the coke formation rate[16]. Moreover, higher catalytic activity over Y zeolite is due to its high surface area which increase the accessibility to acid sites so can improve mass transfer of bulky molecules. Beta zeolite showed prolonged activity, thus until the end of the 210 min, the yield of liquid product increased.

High mesoporous volume and external surface area of Beta zeolite leads to improve mass transfer so prolonging the activity which is compatible with Mirshafiee et al. observations[43].

3.2.2. Liquid product specifications

Results of liquid product analyzes is tabulated in Table 3. Compare with the properties of the feed that listed in Table 1,

Table 2. Pore specifications of three zeolite by N₂ adsorption-desorption analysis

Sample	S _{BET} ^a (m ² /gr)	S _{EXT} ^a (m ² /gr)	S _{mic} ^b (m ² /gr)	V _c ^c (cm ³ /gr)	V _{mic} ^d (cm ³ /gr)	V _{meso} ^e (cm ³ /gr)	Total acid amount (mmol NH ₃ /gr)
Y	812.7	9.0	803.4	0.36	0.34	0.04	1.80
ZSM-5	379.2	15.3	374.8	0.19	0.16	0.02	1.75
Beta	709.0	252.4	456.5	0.95	0.21	0.73	1.29

a external surface area. b micropore surface area. c Volume adsorbed at P/P₀=0.99.
d micropore volume. e Mesopore volume (V_{total}-V_{micro}).

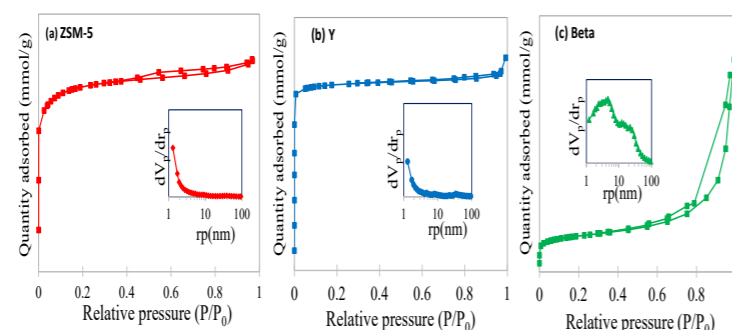


Figure 7. N₂ adsorption-desorption isotherms and BJH pore size distribution (internal) curves of the synthesized samples

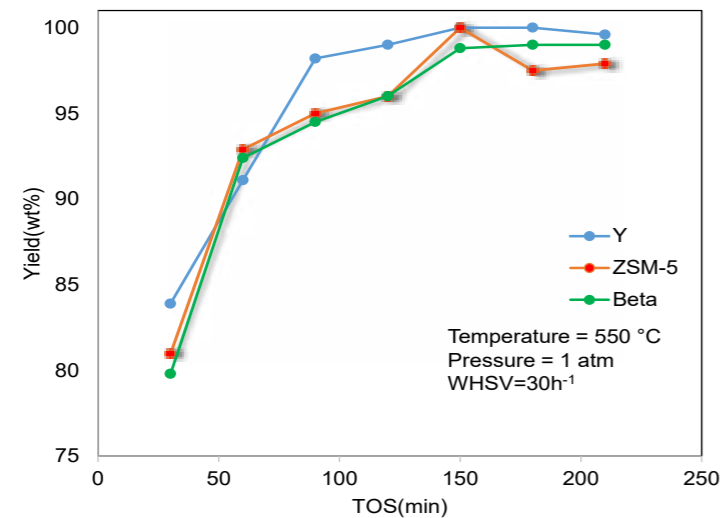


Figure 9. Liquid yield in terms of reaction time for three catalysts

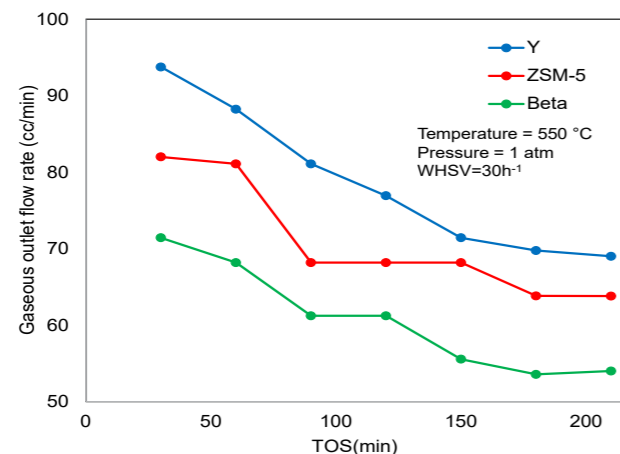


Figure 10. Gaseous yield in terms of reaction time for three catalysts

the average density, viscosity and molecular weight of all catalysts decreased as the lighter compounds are produced during cracking.

Y zeolite remarkably decreased the viscosity of liquid product by 35% compared with the feed. Beta and ZSM-5 zeolites has execute weakly over decreasing the viscosity, due to the higher coke formation on this zeolites.

As the lower the viscosity, the better the quality of the final liquid product, Y zeolite had lower viscosity than the others so had a better cracking performance due to the high surface area which increases accessibility to acid sites and due to the higher total acid sites amount so improve the catalytic performances. Y zeolite is a large pore zeolite(0.74 nm), this makes it possible for heavy molecules with large

diameters to easily pass through these large pores to reach the active sites. so it is very important factor in heavy oil processing [44].

The densities of all of the obtained liquid over three catalysts, decreased compared to the feed which verifies lighter fractions of the liquid product. Y zeolite had lower density than the others which confirms the previous conclusion. Refractive indexes have increased by the ZSM-5>Beta>Y sequences compared to the feed, which is compatible with safari et al. observations[27]. Moreover, lower molecular weight of liquid hydrocarbons compared to the feed, were indicative of obtaining higher yield of lighter components. Y zeolite had the lowest molecular weight among the zeolites. The H/C ratio also increased upon catalytic cracking

over three catalysts, which confirm lighter hydrocarbon production. Y zeolite with better cracking performance, had a higher H/C ratio than the others. Alotaibi et al., also notified in converting heavy residues into lighter products, H/C ratio will increase[1].

Table 3. Properties of liquid product obtained over different zeolites

catalyst	Y	Beta	ZSM-5
Viscosity (cm ² /s) ^a	1.255	1.601	1.828
Molecular Weight ^b	129.69	148.55	158.59
Density (g/cm ³) ^c	0.847	0.862	0.872
Refractive index (n) ^d	1.475	1.478	1.481
H/C Atomic Ratio ^e	7.65	7.64	7.59

^aevaluated by a Liquid viscometer, according to ASTM D7042 standard

^bcalculated by applying Riazi equation

^cmeasured by a 10 ml pycnometer based on ASTM D1480

^ddetermined by using Abbe Refractometer NAR-1T Liquid based on ASTM D1218

^ecalculated by applying Riazi equation

Visual appearance of liquid product obtained after 210 minutes reaction time has been shown in Figure 11. Usually it is said that the lighter cracked products colour, the lighter compounds are in the product which, here, Y zeolite had a lighter colour. In other samples, the variety of colours is due to differences in nature of the products and cokes that deposited in parent catalysts [6].

3.2.3 Spent catalysts characterization

After burning the coked catalysts in furnace during 4hr in 550, weight loss of this spent catalysts are shown in Figure 12. Many factors cause deactivation phenomenon, but the most important factor that has been mentioned a lot in the literatures is the existence of small pores (micropores) in the zeolitic catalysts structure.

When bulky compounds like aromatics with large molecular diameter are formed inside the pores, these can no longer come out of the small pores, so they remains there and cover the active sites, causing the catalyst deactivation[45]. The high surface area of Y zeolite by increasing accessibility to acidic sites creates the expectation that this sample be less prone to coke formation [46]. But as it is clear, weight losses for the Y zeolite was sharper because of its lower Si/Al ratio. The amounts of acid sites, which effect on the deposition of the coke over the catalysts, increase with decrease in the Si/Al ratio, because the number of the acid sites is related to the aluminum content [47] N₂ sorption, NH₃-TPD and Py-FTIR; the intrinsic effect of silicon to aluminum ratio on the selectivity to propene in the conversion of methanol to propene (MTP. So the number of acid sites on Y zeolite based on these explanations as well as the results of Figure 8 and Table 2, is higher than ZSM-5 and Beta zeolites which accelerates the coke formation rate on this sample. So that, even high surface area of Y zeolite is not effective and it is the acidity that prevails and more cokes deposited on this zeolite.

But for Beta and ZSM-5 zeolites, compare with Y zeolite, lower acidity and higher external surface area, are aligned and cause less coke formation. Fu et.al demonstrated higher external surface area leads to formation of more micropores openings exposed on the external surface which inhibits the pore blockage and deactivation of catalyst. On the other hand, large external surface area shorten the diffusion path length, so facilitating the migration of coke precursors inside the micropores to the external surface[46].



Figure 11. Appearance of liquid cracked product obtained after 210 minutes reaction time

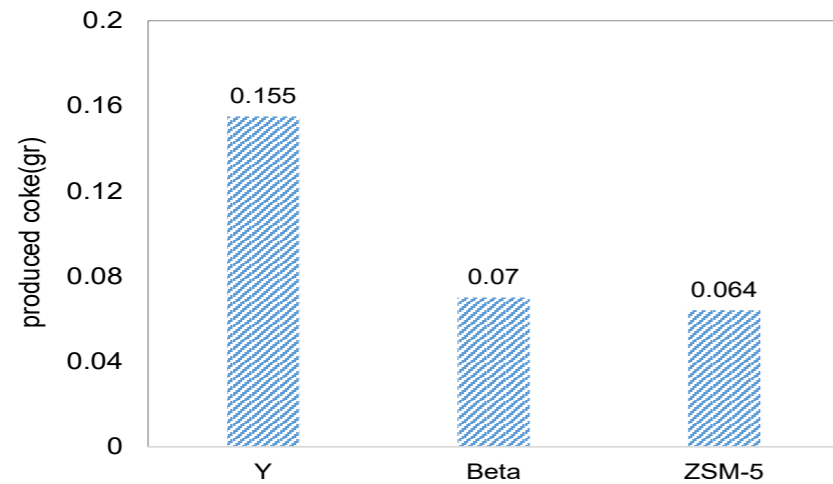


Figure 12. The amount of coke produced during catalytic cracking with different zeolites.

Of course, due to the same effects of dominance of acidity / pore characteristics on each other, there is no significant difference between Beta and ZSM-5 zeolites. Y zeolite, despite producing significant amount of coke, it performed very well in product specifications. The reason can be attributed to the fact that the coke on this zeolite may have been formed at the external surface of the catalyst and so the pores were still accessible and had a little effect on catalyst activity [48]. To determine the molecular structure of deposited coke, studies have been conducted on spent catalysts by FTIR analysis and results are illustrated in Figure 13. As it can be seen, generally both deactivated catalysts and the fresh one, as mentioned in section 3.2.1, have the same trend just the intensity of

some characteristic peaks varies that is due to the impure phase and cokes that appears on parent catalysts during the catalytic test.

Graphitic carbon that shows itself in at 1558 cm^{-1} , was not observed for any of three catalysts [49]. So deposited cokes are not of the graphitic type. Coke with aromatic and olefinic nature can be detected at 1583 cm^{-1} and 1635 cm^{-1} respectively [49]. The highest intensity of these peaks for Y and ZSM-5 zeolites, can represent more production of olefin and aromatic compounds and lower intensity for Beta zeolite can possibly be due to the formation of volatile species which chemically attracted and bonded to the active sites inside the micropore channels of zeolite, resulting in the coke formation [50].

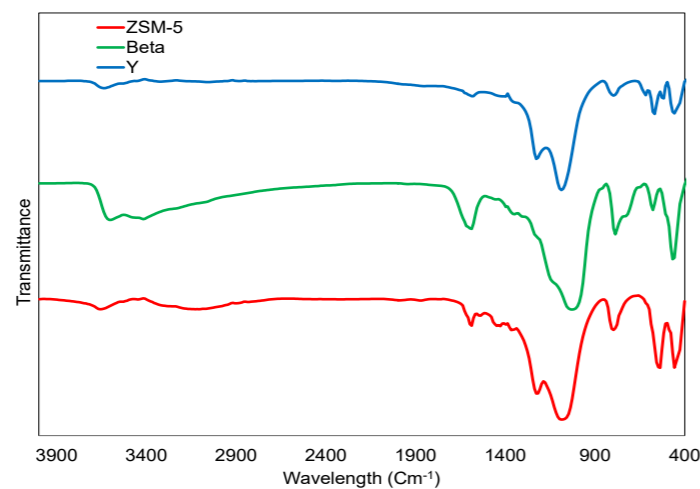


Figure 13. FT-IR spectrum of spent zeolites ZSM-5, Y and Beta

The bands observed at $3000\text{--}3400\text{ cm}^{-1}$ are related to C–H bond stretching vibration in aromatic groups which was absent for these zeolites. So, aromatic rings deposited on these catalysts are unsaturated and poor in hydrogen [17]. Modified Y zeolite with high catalytic activity and long lifetime was successfully prepared using sequential steam-alkali-acid treatments. Different alkali agents (NaOH, Na_2CO_3 and CaCO_3). As mentioned, the band around $3200\text{--}3600\text{ cm}^{-1}$ is attributed to the hydroxyl groups of zeolite which after the reaction, the intensity of the OH groups reduced. It means during the catalytic test, OH groups condensate with coke [17] modified Y zeolite with high catalytic activity and long lifetime was successfully prepared using sequential steam-alkali-acid treatments. Different alkali agents (NaOH, Na_2CO_3 and CaCO_3). On the basis of the observed peak, we can guess with great accuracy that the coke deposited on these catalysts, mostly has an aromatic nature.

4. Conclusion

This study is aimed to compare the catalytic properties and performance of three zeolites containing Y, Beta and ZSM-5. A complete characterization was conducted to have a better insight of their properties and then their performance was tested in the cracking of middle distillate cut "RCD". Summarizing the results of the analyzes and performance test of three catalysts revealed that Y zeolite is more desirable. Better cracking activity, for example decline of viscosity and density of liquid product by 35% and 3% respectively, could be attributed to the higher surface area (from BET results) which increases the accessibility of large molecules to acid sites and due to the higher total acidic sites amount that these acidic sites propel the reaction. However, it should be noted that in terms of coke production, over Beta and ZSM zeolites 50% less coke produced compare with zeolite Y, because they had fewer acid sites, which made them less likely to have coke deposition potential. It seems combining the advantages of two types of molecular sieves as a composite catalyst can improve the catalytic performances.

References

- [1] F. M. Alotaibi et al., "Enhancing the production of light olefins from heavy crude oils: Turning challenges into opportunities," *Catal. Today*, vol. 317, pp. 86–98, 2018, doi: <https://doi.org/10.1016/j.cattod.2018.02.018>.
- [2] L. Huang, W. Guo, P. Deng, Z. Xue, and Q. Li, "Investigation of Synthesizing MCM-41/ZSM-5 Composites," *J. Phys. Chem. B*, vol. 104, no. 13, pp. 2817–2823, Apr. 2000, doi: [10.1021/jp990861y](https://doi.org/10.1021/jp990861y).
- [3] Z. Wang, J. Yu, and R. Xu, "Needs and trends in rational synthesis of zeolitic materials," *Chem. Soc. Rev.*, vol. 41, no. 5, pp. 1729–1741, 2012, doi: [10.1039/C1CS15150A](https://doi.org/10.1039/C1CS15150A).
- [4] J. Qi et al., "Study of cracking of large molecules over a novel mesoporous beta," *Catal. Commun.*, vol. 10, no. 11, pp. 1523–1528, 2009, doi: <https://doi.org/10.1016/j.catcom.2009.04.008>.
- [5] A. Talebian-Kiakalaieh and S. Tarighi, "Synthesis of hierarchical Y and ZSM-5 zeolites using post-treatment approach to maximize catalytic cracking performance," *J. Ind. Eng. Chem.*, vol. 88, pp. 167–177, 2020, doi: <https://doi.org/10.1016/j.jiec.2020.04.009>.
- [6] U. Khalil et al., "Robust surface-modified Beta zeolite for selective production of lighter fuels by steam-assisted catalytic cracking from heavy oil," *Fuel*, vol. 168, pp. 61–67, 2016, doi: <https://doi.org/10.1016/j.fuel.2015.11.085>.
- [7] L. Zhao, J. Gao, C. Xu, and B. Shen, "Alkali-treatment of ZSM-5 zeolites with different SiO₂/Al₂O₃ ratios and light olefin production by heavy oil cracking," *Fuel Process. Technol.*, vol. 92, no. 3, pp. 414–420, 2011, doi: <https://doi.org/10.1016/j.fuproc.2010.10.003>.
- [8] X. Gao et al., "High silica REHY zeolite with low rare earth loading as high-performance catalyst for heavy oil conversion," *Appl. Catal. A Gen.*, vol. 413–414, pp. 254–260, 2012, doi: <https://doi.org/10.1016/j.apcata.2011.11.015>.
- [9] K. Zhang, S. Fernandez, E. S. Converse, and S. Kobaslija, "Exploring the impact of synthetic strategies on catalytic cracking in hierarchical beta zeolites via hydrothermal desilication and organosilane-templated synthesis," *Catal. Sci. Technol.*, vol. 10, no. 14, pp. 4602–4611, 2020, doi: [10.1039/D0CY01209B](https://doi.org/10.1039/D0CY01209B).
- [10] K. T. Thomson, "Handbook of Zeolite Science and Technology Edited by Scott M. Auerbach (University of Massachusetts, Amherst), Kathleen A. Carrado (Argonne National Laboratory), Prabir K. Dutta (The Ohio State University). Marcel Dekker, Inc.: New York, Basel, 2003. xi," *J. Am. Chem. Soc.*, vol. 126, no. 28, pp. 8858–8859, Jul. 2004, doi: [10.1021/ja0336067](https://doi.org/10.1021/ja0336067).
- [11] W. Lutz, "Zeolite Y: Synthesis, Modification, and Properties—A Case Revisited," *Adv. Mater. Sci. Eng.*, vol. 2014, p. 724248, 2014, doi: [10.1155/2014/724248](https://doi.org/10.1155/2014/724248).
- [12] J. García-Martínez, K. Li, and G. Krishnaiah, "A mesostructured Y zeolite as a superior FCC catalyst – from lab to refinery," *Chem. Commun.*, vol. 48, no. 97, pp. 11841–11843, 2012, doi: [10.1039/C2CC35659G](https://doi.org/10.1039/C2CC35659G).
- [13] Y. Zhao et al., "Synthesis, characterization, and catalytic performance of high-silica Y zeolites with different crystallite size," *Microporous Mesoporous Mater.*, vol. 167, pp. 102–108, Feb. 2013, doi: [10.1016/j.micromeso.2012.03.016](https://doi.org/10.1016/j.micromeso.2012.03.016).
- [14] Z. Qin et al., "A defect-based strategy for the preparation of mesoporous zeolite Y for high-performance catalytic cracking," *J. Catal.*, vol. 298,

- pp. 102–111, 2013, doi: <https://doi.org/10.1016/j.jcat.2012.11.023>.
- [15] W. Li, J. Zheng, Y. Luo, C. Tu, Y. Zhang, and Z. Da, "Hierarchical Zeolite Y with Full Crystallinity: Formation Mechanism and Catalytic Cracking Performance," *Energy & Fuels*, vol. 31, no. 4, pp. 3804–3811, Apr. 2017, doi: [10.1021/acs.energyfuels.6b03421](https://doi.org/10.1021/acs.energyfuels.6b03421).
- [16] S. Oruji, R. Khoshbin, and R. Karimzadeh, "Combination of precipitation and ultrasound irradiation methods for preparation of lanthanum-modified Y zeolite nano-catalysts used in catalytic cracking of bulky hydrocarbons," *Mater. Chem. Phys.*, vol. 230, pp. 131–144, 2019, doi: <https://doi.org/10.1016/j.matchemphys.2019.03.038>.
- [17] E. Aghaei, R. Karimzadeh, H. R. Godini, A. Gurlo, and O. Gorke, "Improving the physicochemical properties of Y zeolite for catalytic cracking of heavy oil via sequential steam-alkali-acid treatments," *Microporous Mesoporous Mater.*, vol. 294, p. 109854, 2020, doi: <https://doi.org/10.1016/j.micromeso.2019.109854>.
- [18] J. B. Higgins et al., "The framework topology of zeolite beta," *Zeolites*, vol. 8, no. 6, pp. 446–452, 1988, doi: [https://doi.org/10.1016/S0144-2449\(88\)80219-7](https://doi.org/10.1016/S0144-2449(88)80219-7).
- [19] Z. Huang, J.-F. Su, Y.-H. Guo, X.-Q. Su, and L.-J. Teng, *Synthesis of well-crystallized zeolite beta at large scale and its incorporation into polysulfone matrix for gas separation*, vol. 196, 2009.
- [20] Y. J. Lee, J.-H. Kim, S. H. Kim, S. B. Hong, and G. Seo, "Nanocrystalline beta zeolite: An efficient solid acid catalyst for the liquid-phase degradation of high-density polyethylene," *Appl. Catal. B Environ.*, vol. 83, no. 1, pp. 160–167, 2008, doi: <https://doi.org/10.1016/j.apcatb.2008.02.013>.
- [21] A. Corma, V. Fornes, F. Melo, and J. Pérez-Pariente, *Zeolite Beta: Structure, Activity, and Selectivity for Catalytic Cracking*, vol. 375, 1988.
- [22] P. G. Smirniotis and E. Ruckenstein, "Comparison of the Performance of ZSM-5, .beta. Zeolite, Y, USY, and Their Composites in the Catalytic Cracking of n-Octane, 2,2,4-Trimethylpentane, and 1-Octene," *Ind. Eng. Chem. Res.*, vol. 33, no. 4, pp. 800–813, Apr. 1994, doi: [10.1021/ie00028a004](https://doi.org/10.1021/ie00028a004).
- [23] T. F. Degnan, G. K. Chitnis, and P. H. Schipper, "History of ZSM-5 fluid catalytic cracking additive development at Mobil," *Microporous Mesoporous Mater.*, vol. 35–36, pp. 245–252, 2000, doi: [https://doi.org/10.1016/S1387-1811\(99\)00225-5](https://doi.org/10.1016/S1387-1811(99)00225-5).
- [24] Y. Ji, H. Yang, Q. Zhang, and W. Yan, "Phosphorus modification increases catalytic activity and stability of ZSM-5 zeolite on supercritical catalytic cracking of n-dodecane," *J. Solid State Chem.*, vol. 251, pp. 7–13, 2017, doi: [10.1016/j.jssc.2017.03.023](https://doi.org/10.1016/j.jssc.2017.03.023).
- [25] O. Awayssa, N. Al-Yassir, A. Aitani, and S. Al-Khattaf, "Modified HZSM-5 as FCC additive for enhancing light olefins yield from catalytic cracking of VGO," *Appl. Catal. A Gen.*, vol. 477, pp. 172–183, 2014, doi: <https://doi.org/10.1016/j.apcata.2014.03.021>.
- [26] A. Ishihara, K. Kimura, A. Owaki, K. Inui, T. Hashimoto, and H. Nasu, "Catalytic cracking of VGO by hierarchical ZSM-5 zeolite containing mesoporous silica-aluminas using a Curie point pyrolyzer," *Catal. Commun.*, vol. 28, pp. 163–167, 2012, doi: <https://doi.org/10.1016/j.catcom.2012.08.023>.
- [27] S. Safari, R. Khoshbin, and R. Karimzadeh, "Catalytic upgrading of heavy oil over mesoporous HZSM-5 zeolite in the presence of atmospheric oxygen flow," *React. Kinet. Mech. Catal.*, vol. 129, no. 2, pp. 941–962, 2020, doi: [10.1007/s11144-020-01731-w](https://doi.org/10.1007/s11144-020-01731-w).
- [28] H. Hattori and Y. Ono, "4 - Catalysts and catalysis for acid–base reactions," in *Metal Oxides*, J. C. B. T.-M. O. in H. C. Védrine, Ed. Elsevier, 2018, pp. 133–209.
- [29] T. Albayati and A. Doyle, "Purification of aniline and nitrosubstituted aniline contaminants from aqueous solution using beta zeolite," *Chemistry (Easton)*, vol. 23, pp. 105–114, Jan. 2014.
- [30] S. Xu et al., "Advances in Catalysis for Methanol-to-Olefins Conversion," in *Advances in Catalysis*, 2017.
- [31] M. Riazi, *Characterization and Properties of Petroleum Fractions*, 1st ed. 2005.
- [32] N. Taufiqurrahmi, A. R. Mohamed, and S. Bhatia, "Nanocrystalline zeolite beta and zeolite Y as catalysts in used palm oil cracking for the production of biofuel," *J. Nanoparticle Res.*, vol. 13, no. 8, pp. 3177–3189, 2011, doi: [10.1007/s11051-010-0216-8](https://doi.org/10.1007/s11051-010-0216-8).
- [33] L. Mu, W. Feng, H. Zhang, X. Hu, and Q. Cui, "Synthesis and catalytic performance of a small crystal NaY zeolite with high SiO₂/Al₂O₃ ratio," *RSC Adv.*, vol. 9, no. 36, pp. 20528–20535, 2019, doi: [10.1039/C9RA03324F](https://doi.org/10.1039/C9RA03324F).
- [34] S. Zhang et al., "OSDA-free synthesis of zeolite beta by magadiite hydrothermal conversion method and an insight into the changes of medium-range structure during crystallization," *Microporous Mesoporous Mater.*, vol. 278, pp. 81–90, 2019, doi: <https://doi.org/10.1016/j.micromeso.2018.11.028>.
- [35] G. Song et al., "Synthesis and Characterization of Hierarchical ZSM-5 Zeolites with Outstanding Mesoporosity and Excellent Catalytic Properties," *Nanoscale Res. Lett.*, vol. 13, no. 1, p. 364, 2018, doi: [10.1186/s11671-018-2779-8](https://doi.org/10.1186/s11671-018-2779-8).
- [36] R. Martínez-Franco, C. Paris, M. E. Martínez-Armero, C. Martínez, M. Moliner, and A. Corma, "High-silica nanocrystalline Beta zeolites: efficient synthesis and catalytic application," *Chem. Sci.*, vol. 7, no. 1, pp. 102–108, 2016, doi: [10.1039/C5SC03019F](https://doi.org/10.1039/C5SC03019F).
- [37] R. Ravandi, R. Khoshbin, and R. Karimzadeh, "Synthesis of free template ZSM-5 catalyst from rice husk ash and co-modified with lanthanum and phosphorous for catalytic cracking of naphtha," *J. Porous Mater.*, vol. 25, no. 2, pp. 451–461, Apr. 2018, doi: [10.1007/s10934-017-0457-3](https://doi.org/10.1007/s10934-017-0457-3).
- [38] J. Plana-Pallejà, S. Abelló, C. Berruoco, and D. Montané, "Effect of zeolite acidity and mesoporosity on the activity of Fischer–Tropsch Fe/ZSM-5 bifunctional catalysts," *Appl. Catal. A Gen.*, vol. 515, pp. 126–135, 2016, doi: <https://doi.org/10.1016/j.apcata.2016.02.004>.
- [39] K. Zhang, S. Fernandez, J. A. Lawrence, and M. L. Ostraat, "Organotemplate-Free β Zeolites: From Zeolite Synthesis to Hierarchical Structure Creation," *ACS Omega*, vol. 3, no. 12, pp. 18935–18942, 2018, doi: [10.1021/acsomega.8b02762](https://doi.org/10.1021/acsomega.8b02762).
- [40] A. Bazyari, A. A. Khodadadi, N. Hosseinpour, and Y. Mortazavi, "Effects of steaming-made changes in physicochemical properties of Y-zeolite on cracking of bulky 1,3,5-triisopropylbenzene and coke formation," *Fuel Process. Technol.*, vol. 90, pp. 1226–1233, Oct. 2009, doi: [10.1016/j.fuproc.2009.06.002](https://doi.org/10.1016/j.fuproc.2009.06.002).
- [41] S. Sukanuma, H. Zhang, C. Yang, F.-S. Xiao, and N. Katada, "Acidic property of BEA zeolite synthesized by seed-directed method," *J. Porous Mater.*, vol. 23, no. 2, pp. 415–421, 2016, doi: [10.1007/s10934-015-0095-6](https://doi.org/10.1007/s10934-015-0095-6).
- [42] S. Safari, R. Khoshbin, and R. Karimzadeh, "Beneficial use of ultrasound irradiation in synthesis of beta-clinoptilolite composite used in heavy oil upgrading process," *RSC Adv.*, vol. 9, no. 29, pp. 16797–16811, 2019, doi: [10.1039/c9ra02173f](https://doi.org/10.1039/c9ra02173f).
- [43] F. Mirshafiee, R. Karimzadeh, and R. Khoshbin, "Free template synthesis of novel hybrid MFI/BEA zeolite structure used in the conversion of methanol to clean gasoline: Effect of Beta zeolite content," *Fuel*, vol. 304, p. 121386, 2021, doi: <https://doi.org/10.1016/j.fuel.2021.121386>.
- [44] C. Nguyen-Huy and E. Shin, "Hierarchical macro-mesoporous Al₂O₃-supported NiK catalyst for steam catalytic cracking of vacuum residue," *Fuel*, vol. 169, pp. 1–6, Apr. 2016, doi: [10.1016/j.fuel.2015.11.088](https://doi.org/10.1016/j.fuel.2015.11.088).
- [45] S. M. H. Al Wahabi, "Conversion of methanol to light olefins on SAPO-34: kinetic modeling and reactor design," Feb. 2005.
- [46] T. Fu, J. Chang, J. Shao, and Z. Li, "Fabrication of a nano-sized ZSM-5 zeolite with intercrystalline mesopores for conversion of methanol to gasoline," *J. Energy Chem.*, vol. 26, no. 1, pp. 139–146, Jan. 2017, doi: [10.1016/j.jechem.2016.09.011](https://doi.org/10.1016/j.jechem.2016.09.011).
- [47] H. HUANG, H. ZHU, S. ZHANG, Q. ZHANG, and C. LI, "Effect of silicon to aluminum ratio on the selectivity to propene in methanol conversion over H-ZSM-5 zeolites," *J. Fuel Chem. Technol.*, vol. 47, no. 1, pp. 74–82, 2019, doi: [https://doi.org/10.1016/S1872-5813\(19\)30005-2](https://doi.org/10.1016/S1872-5813(19)30005-2).
- [48] S. Müller et al., "Coke formation and deactivation pathways on H-ZSM-5 in the conversion of methanol to olefins," *J. Catal.*, vol. 325, pp. 48–59, 2015, doi: <https://doi.org/10.1016/j.jcat.2015.02.013>.
- [49] S. Abbasizadeh and R. Karimzadeh, "Effect of Next-Nearest-Neighbor Aluminum Atoms in the HZSM-5 Framework Synthesized with Various Aluminum Sources on Liquefied Petroleum Gas Transformation to Light Olefins," *Ind. Eng. Chem. Res.*, vol. 57, no. 23, pp. 7783–7794, Jun. 2018, doi: [10.1021/acs.iecr.8b00951](https://doi.org/10.1021/acs.iecr.8b00951).
- [50] Z. Wan, G. K. Li, C. Wang, H. Yang, and D. Zhang, "Relating coke formation and characteristics to deactivation of ZSM-5 zeolite in methanol to gasoline conversion," *Appl. Catal. A Gen.*, vol. 549, pp. 141–151, 2018, doi: [10.1016/j.apcata.2017.09.035](https://doi.org/10.1016/j.apcata.2017.09.035).

تأثیر خواص بافتی زئولیت های Y، ZSM-5 و بتا بر روی خواص کاتالیستی آنها در فرایند شکست کاتالیستی برش میان تقطیر RCD

سیده فائزه میرشفیعی^۱، رامین کریم زاده^{۲*}، رضا خوشبین^۳

۱. دانشجوی دکتری، دانشکده مهندسی شیمی، دانشگاه تربیت مدرس، تهران

۲. عضو هیئت علمی، دانشکده مهندسی شیمی، دانشگاه تربیت مدرس، تهران

۳. دانشگاه بین المللی امام خمینی (ره)، مرکز آموزش عالی فنی و مهندسی بویین زهرا، قزوین

چکیده

در مطالعه حاضر، عملکرد سه کاتالیست شامل زئولیت های Y، ZSM-5 و بتا در کراکینگ کاتالیستی یک برش میانی مورد مطالعه قرار گرفت. برای تعیین مشخصات کاتالیست ها از آنالیزهای XRD، FTIR، SEM و BET استفاده شده است. همچنین کاتالیستهای مستعمل از منظر نوع و مقدار کک جمع یافته مورد تحلیل و بررسی قرار گرفتند. نتیجه تست های راکتوری نشان داد که زئولیت Y عملکرد بهتری از خود به نمایش گذاشت به طوری که که ویسکوزیته و دانسیته محصول مایع را به ترتیب ۵۳٪ و ۳٪ کاهش داد اما کک تشکیل شده بر روی این زئولیت ۰۵٪ بیشتر از زئولیت های ZSM-5 و بتا بوده است. در نهایت، نتایج نشان داده اند در کراکینگ هیدروکربنهای سنگین، عملکرد نهایی کاتالیست به اثرات هم افزای ساختار حفرات کاتالیست و اسیدیته آن وابسته است.

مشخصات مقاله

تاریخچه مقاله:

دریافت: ۲۲ اسفند ۱۳۹۹

دریافت پس از اصلاح: ۳۱ مرداد ۱۴۰۰

پذیرش نهایی: ۱۳ آبان ۱۴۰۰

کلمات کلیدی:

کراکینگ کاتالیستی

هیدروکربن های سنگین

زئولیت Y

زئولیت ZSM-5

زئولیت Beta

*عهدمدار مکاتبات: رامین کریم زاده

رایانامه: Ramin@modares.ac.ir
r.khoshbin@bzeng.ikiu.ac.ir

تلفن: ۰۲۱۸۲۸۸۳۳۱۵

نحوه استناد به این مقاله:

Mirshafiee F, Karimzadeh R, Khoshbin R, Effect of Textural Properties of Y, ZSM-5 and Beta Zeolites on Their Catalytic Activity in Catalytic Cracking of a Middle Distillate Cut Named RCD, Journal of Oil, Gas and Petrochemical Technology, 2021; 8(2): -74. DOI:10.22034/JOGPT.2022.273313.1092.